Published in final edited form as:
J Am Chem Soc. 2012 October 24; 134(42): 17428–17431. doi:10.1021/ja308203h.

Fluorogenic Azidofluoresceins for Biological Imaging

Peyton Shieh[†,¥], **Matthew J. Hangauer**[†,¥,¦], and **Carolyn R. Bertozzi**[†,‡,§,*]

[†]Department of Chemistry, University of California, Berkeley, California 94720, United States

[‡]Department of Molecular and Cell Biology, University of California, Berkeley, California 94720, United States

[§]Howard Hughes Medical Institute, University of California, Berkeley, California 94720, United States

Abstract

Fluorogenic probes activated by bioorthogonal chemical reactions can enable biomolecule imaging in situations where it is not possible to wash away unbound probe. One challenge for the development of such probes is the *a priori* identification of structures that will undergo a dramatic fluorescence enhancement by virtue of the chemical transformation. With the aid of density functional theory calculations reported previously by Nagano and coworkers, we identified azidofluorescein derivatives that were predicted to undergo an increase in fluorescence quantum yield upon Cu-catalyzed or Cu-free cycloaddition with linear or cyclic alkynes, respectively. Four derivatives were experimentally verified in model reactions, and one, a 4-azidonaphthyl fluorescein analog, was further shown to label alkyne-functionalized proteins *in vitro* and glycoproteins on cells with excellent selectivity. The azidofluorescein derivative also enabled cell imaging under no-wash conditions with good signal above background. This work establishes a platform for the rational design of fluorogenic azide probes with spectral properties tailored for biological imaging.

Bioorthogonal chemistry has enabled the visualization and study of biomolecules that cannot be tagged with genetically encoded fluorescent proteins.[1] Much work has been devoted to expanding the toolbox of bioorthogonal reactions, and these efforts can be complemented by the development of fluorogenic probes.[2] Such probes are typically endowed with a functionality that suppresses fluorescence. Its transformation during the reaction creates a new functionality that no longer quenches fluorescence of the underlying system, resulting in a fluorescence enhancement. Such probes offer significant advantages for imaging studies where it is not possible to wash away unreacted probe, such as real-time imaging of dynamic processes in cells or visualization of molecules in live organisms.

One of the most widely used bioorthogonal reactions is the azide-alkyne [3+2] cycloaddition to form a triazole. This reaction has enabled the selective visualization of azide- or alkyne-labeled proteins, glycans, nucleic acids, and lipids.[3] Several azide-[4–7] and alkyne[7–11]-functionalized fluorogenic probes have been reported, largely based on coumarins[4,8], naphthalimides[7] and other systems that require UV excitation and emit blue light.[5,10,11] Such wavelengths are not ideal for biological imaging due to high levels of autofluorescence and poor tissue penetrance.[13]

[*]Corresponding Author: crb@berkeley.edu.
[¥]Equal contribution
[¦]Present Address: School of Medicine, University of California, San Francisco

Supporting Information. Experimental and synthetic procedures, materials, and supporting figures and tables. This material is available free of charge via the Internet at http://pubs.acs.org.

An obvious improvement upon these designs would be the development of azido or alkynyl fluorogenic probes with longer excitation and emission wavelengths. Some attempts at achieving this goal have been made. Recently, an azido BODIPY probe was reported, but the compound was unstable and unable to specifically react with alkynes on cellular biolmolecules.[6] An alkynyl benzothiazole analog that emits at ~500 nm has been reported but its fluorescence enhancement upon reaction with azides was a modest 3.5-fold in aqueous buffer.[11] A screen of 200 combinations of various alkynyl xanthenes and organic azides produced two reagent pairs that reacted to give a fluorescence enhancement of 10-fold in organic solvent.[12] The utility of these alkyne/azide pairs in biological settings remains unclear. Thus, fluorogenic azido or alkynyl probes that perform well as cell imaging reagents remain an important goal.

Here we report the rational design and experimental validation of azide-functionalized fluorogenic probes based on the widely-used blue-excitation green-emission fluorescein scaffold. Our design capitalized on a theoretical model developed by Nagano and coworkers that enables prediction of fluorescence quantum yield based on density functional theory calculations.[14] Nagano demonstrated that the pendant aryl ring of fluorescein can quench fluorescence via photoinduced electron transfer.[15] This quenching can be increased or decreased in a predictable manner by altering the electron density of the aryl ring using various substituents. More importantly, Nagano and coworkers also demonstrated a direct relationship between experimentally determined fluorescence quantum yield and the calculated HOMO energy (E_{HOMO}) of the pendant aryl ring at the B3LYP/6-31G(d) level of theory. Thus, in principle, by calculating the E_{HOMO} values of the aryl ring, one can predict the fluorescence quantum yield of the corresponding fluorescein and identify suitable targets for experimental evaluation. This insight has guided the design of other activatable fluorescein-based probes.[16,17]

Applying this concept to the development of a fluorogenic azidofluorescein, we performed computational analyses of a panel of fluorescein analogs in which the azide group was directly appended to a variety of aryl substituents (Table S1). We anticipated that triazole formation would lower the aryl E_{HOMO} value relative to that of the azide-functionalized substrate, reducing photoinduced electron transfer and resulting in fluorescence turn-on (Figure 1). We focused our analysis on targets that could be readily synthesized from commercially available bromo- or iodoaryl starting materials with a substituent ortho to the halogen.[18] Table S1 shows the 15 analogs chosen for computational studies as well as the E_{HOMO} values of the aryl azides and corresponding triazoles calculated at the B3LYP 6-31G(d) level of theory.

Calculations indicated that all compounds, with one exception, undergo the expected decrease in aryl E_{HOMO} value upon triazole formation. From these compounds, four (**1–4**, Fig. 1b) were chosen as targets for synthesis and further evaluation. These candidates possessed azide E_{HOMO} values of −0.196 to −0.210 Hartrees and triazole E_{HOMO} values of −0.203 to −0.220 Hartrees. Given the relationship between fluorescence quantum yield and E_{HOMO} value, we anticipated that compounds **1**–**4** would undergo an increase in fluorescence quantum yield at pH 7.4 upon triazole formation.[19]

Compounds **1**, **2** and **3** were prepared by addition of the corresponding aryl organolithium compound to a protected xanthone derivative, an approach reported previously by Tsien and coworkers (Scheme 1).[22] To generate compound **1**, we subjected commercially available bromoaniline **6** to diazotization and then protected the diazonium group by reaction with pyrrolidine,[20,21] affording aryl triazene **7**. The aryl triazene underwent lithium halogen exchange and addition to bis-TBS-protected xanthone **5**[22] to afford fluorescein derivative **8**. Treatment of this compound with acid unmasked the diazonium group, which was displaced

by azide anion to afford azidofluorescein **1**. Using this same strategy, azidofluoresceins **2** and **3** were prepared (see Supporting Information). Attempts to convert 4-bromo-6-aminoindole, the starting material for compound **4**, to the corresponding triazene were unsuccessful.[23] Instead, we opted to start from acetylated indole **10**, prepared from known compound **9** by iron reduction and acetylation in acetic acid (Scheme 2). In one pot, we treated **10** with two equivalents of sodium hydride, then with *tert*-butyllithium to effect lithium halogen exchange; coupling with **5**, afforded, after acid workup, compound **11**. Deacetylation using BF_3-OEt_2 in MeOH[24], diazotization, and azide displacement afforded the desired azidofluorescein **4**.

To synthesize the triazole products for photophysical measurements, azidofluoresceins **1–4** were further reacted with model alkynes **12–**14 (Figure 2) under Cu-catalyzed (for compound **12**) or Cu-free (**13** [also abbreviated DIFO] and **14** [DIMAC]) conditions.[25,26] The fluorescence quantum yields of all compounds were then measured in pH 7.4 phosphate-buffered saline (PBS) (Table 1).[27] Each triazolylfluorescein showed an increase in fluorescence quantum yield compared to the parent azidofluorescein. The relationship between fluorescence quantum yield and calculated E_{HOMO} followed a trend similar to that observed by Nagano (Figure 2). As a point of comparison, we analyzed known 5-azidofluorescein (N_3-fluor, Table 1), which is currently used as an alkyne-specific probe but is not reported to be fluorogenic.[28,29] The calculated E_{HOMO} values of 5-azidofluorescein and its corresponding triazole product with **12** were −0.242 and −0.246 Hartrees, respectively, suggesting that both compounds should be highly fluorescent. Consistent with prediction, we found the two compounds to have fluorescent quantum yields of 0.75 and 0.59, respectively.

Interestingly, the fluorescence enhancement of **1–4** upon triazole formation was dependent on the structure of the alkyne substrate, but not in a systematic way. Presumably, structure-dependent pathways for nonradiative decay contribute to the observed fluorescence of the triazole products. Nonetheless, half of the azidofluorescein- alkyne pairs gave a fluorescence turn-on of >10-fold, indicating that rational design principles can more efficiently identify fluorogenic reagent pairs than undirected screening approaches.

Of the reagents tested, azidofluorescein **1** gave the highest and most alkyne-independent increase in fluorescence quantum yield at pH 7.4. Thus, we chose to further evaluate its use in biological labeling. First, we performed a model reaction with alkyne **12** under standard biological labeling conditions ($CuSO_4$, ligand,[30,31] and sodium ascorbate). The expected fluorescence increase was observed and the reaction was complete within 1 h (Figure S2). We next demonstrated that azidofluorescein **1** can selectively label alkyne-tagged proteins. Bovine serum albumin (BSA) was functionalized with alkynes by modification of its lysine side chains with 4-pentynoyl-NHS-ester. An alkene-modified control sample was produced by reaction of BSA with 4-pentenoyl-NHS ester. Alkyne- or alkene-modified BSA, as well as unmodified BSA, were incubated with **1**, $CuSO_4$, TBTA, and sodium ascorbate in 95:5 pH 7.4 PBS/*tert*-butanol, and the samples were analyzed by SDS-PAGE. Fluorescence scanning showed that only alkyne-modified BSA was chemically labeled, and in a Cu-dependent manner (Figure S3).

To evaluate azidofluorescein **1** as a biological imaging reagent, Chinese Hamster Ovary (CHO) cells were metabolically labeled with peracetylated *N*-(4-pentynoyl)mannosamine (Ac_4ManNAl) (50 μM for 3 days) as previously described.[32] These cells convert Ac_4ManNAl to the corresponding alkynyl-sialic acid, which is then incorporated into cell-surface glycoproteins. Control cells were incubated with peracetylated *N*-acetylmannosamine (Ac_4ManNAc). The cells were then fixed with paraformaldehyde and incubated with compound **1**, $CuSO_4$, sodium ascorbate, and TBTA for 1 h. After washing,

the cells showed robust alkyne-dependent labeling with **1** (Figure S4). The experiment was then repeated, but without the washing step after reaction with **1**. As shown in Figure 4, bright cell-surface fluorescence was observed for alkyne-labeled cells (Fig. 4b) compared to the background observed with control (Ac_4ManNAc-labeled) cells (Fig. 4d). By contrast, whereas non-fluorogenic 5-azidofluorescein also labels cells in an alkyne-dependent manner (Figure S5), the strong fluorescence signal of this azide dye gave high background under no-wash conditions (Figure 4f), thereby obscuring cell-surface labeling of alkynyl sugars.

A potential problematic side reaction of aryl azides is their reduction to the corresponding anilines by endogenous thiols. This reaction has been demonstrated to proceed under physiological conditions,[33] and indeed it undermined the use of azidonaphthalimides as biological imaging reagents.[7] Aryl azide reduction has also been used to detect intracellular hydrogen sulfide.[34] Calculations indicate that this reduction pathway would not be an issue for **1**, as the predicted aryl E_{HOMO} value of the aniline reduction product is higher than that of the starting aryl azide (−0.189 Hartrees vs. −0.210 Hartrees). To demonstrate this experimentally, we reduced **1** with dithiothreitol and measured the fluorescence quantum yield of the arylamine product. As expected, reduction resulted in a decrease in fluorescent quantum yield at pH 7.4 from 0.024 to 0.0067, indicating that, if this side reaction occurs *in vivo*, it would not contribute significantly to background fluorescence.

In summary, by taking advantage of the observed relationship between E_{HOMO} of a pendant aryl substituent and fluorescence quantum yield, we were able to identify potential fluorogenic azidofluoresceins. One azidofluorescein, **1**, was suitable for no-wash imaging of cells. This compound is cell permeable and may be suitable for intracellular imaging of biomolecule-associated cyclooctynes as well (Figure S6). We anticipate that this general strategy will be useful for the development of fluorogenic alkynyl fluorescein analogs as well. Indeed, calculations indicate that conversion of aryl alkynes to the corresponding triazoles results in a significant increase in E_{LUMO}. In principle, alkynyl fluoresceins that are internally quenched by PET, in this case from the xanthene to the aryl ring, should undergo fluorescence enhancement upon triazole formation.[35] This notion, as well as extension of the design principle to red-shifted fluorophores, are interesting future directions.

Supplementary Material

Refer to Web version on PubMed Central for supplementary material.

Acknowledgments

This work was funded by NIH grant GM58867 to C.R.B. We would like to thank Prof. C. Chang (UC Berkeley) for the generous use of his fluorimeter. M.J.H. was supported by a National Defense Science and Engineering Graduate Fellowship.

References

1. For a general review of bioorthogonal chemistry, see: Sletten EM, Bertozzi CR. Angew Chem Int Ed. 2009; 48:6974–6998.
2. For a review on fluorogenic click probes, see: Le Droumaguet C, Wang C, Wang Q. Chem Soc Rev. 2010; 39:1233–1239. [PubMed: 20309483]
3. For reviews on applications of the azide-alkyne [3+2] cycloaddition in chemical biology, see: Best MD. Biochemistry. 2009; 48:6571–6584. [PubMed: 19485420] Jewett JC, Bertozzi CR. Chem Soc Rev. 2010; 39:1272–1279. [PubMed: 20349533]
4. Sivakumar K, Xie F, Cash BM, Long S, Barnhill HN, Wang Q. Org Lett. 2004; 6:4603–4606. [PubMed: 15548086]

5. Xie F, Sivakumar K, Zeng QB, Bruckman MA, Hodges B, Wang Q. Tetrahedron. 2008; 64:2906–2914.
6. Wang C, Xie F, Suthiwangcharoen N, Sun J, Wang Q. Sci China Chem. 2012; 55:125–130.
7. Sawa M, Hsu TL, Itoh T, Sugiyama M, Hanson SR, Vogt PK, Wong CH. Proc Natl Acad Sci. 2006; 103:12371–12376. [PubMed: 16895981]
8. Zhou Z, Fahrni CJ. J Am Chem Soc. 2004; 126:8862–8863. [PubMed: 15264794]
9. Jewett JC, Bertozzi CR. Org Lett. 2011; 13:5937–5939. [PubMed: 22029411]
10. Key JA, Cairo CW. Dyes and Pigments. 2010; 88:95–102.
11. Qi J, Han MS, Chang YC, Tung CH. Bioconj Chem. 2011; 22:1758–1762.
12. Li J, Hu M, Yao SQ. Org Lett. 2009; 11:3008–3011. [PubMed: 19522535]
13. Weissleder R, Ntziachristos V. Nature Medicine. 2003; 9:123–128.
14. Urano Y, Kamiya M, Kanda K, Ueno T, Hirose K, Nagano T. J Am Chem Soc. 2005; 127:4888–4894. [PubMed: 15796553]
15. Miura T, Urano Y, Tanaka K, Nagano T, Ohkubo K, Fukuzumi S. J Am Chem Soc. 2003; 125:8666–8671. [PubMed: 12848574]
16. Kamiya M, Kobayashi H, Hama Y, Bernardo M, Nagano T, Choyke PL, Urano Y. J Am Chem Soc. 2007; 129:3918–3929. [PubMed: 17352471]
17. Kobayashi T, Urano Y, Kamiya M, Ueno T, Kojima H, Nagano T. J Am Chem Soc. 2007; 129:6696–6697. [PubMed: 17474746]
18. This ortho substituent restricts rotation around the C_{aryl}-C_{aryl} bond and is necessary for maintaining predictable fluorescence quantum yields (See ref 14).
19. Nagano and coworkers have shown that while the general trend relating E_{HOMO} to quantum yield is similar at different pH values, the exact E_{HOMO} values at which fluorescence dramatically increases are pH-dependent (See ref 14). We performed our calculations with the anionic form of fluorescein, which should predominate at physiological pH.
20. Gross ML, Blank DH, Welch WM. J Org Chem. 1993; 58:2104–2109.
21. Liu CY, Knochel P. J Org Chem. 2007; 72:7106–7115. [PubMed: 17705535]
22. Mintaz AK, Kao JPY, Tsien RY. J Biol Chem. 1989; 265:8171–8178.
23. For another example of an unsuccessful attempt at triazene formation from aminoindoles, see: Cirrincione G, Almerico AM, Dattolo G, Aiello E, Diana P, Grimaudo S, Barraja P, Mingoia F, Gancitano RA. Eur J Med Chem. 1994; 29:889–891.
24. Miltsov S, Rivera L, Encinas C, Alonso J. Tet Lett. 2003; 44:2301–2303.
25. Baskin JM, Prescher JA, Laughlin ST, Agard NJ, Chang PV, Miller IA, Lo A, Codelli JA, Bertozzi CR. Proc Natl Acad Sci. 2007; 104:16793–16797. [PubMed: 17942682]
26. Sletten E, Bertozzi CR. Org Lett. 2008; 10:3097–3099. [PubMed: 18549231]
27. The values we measured were, on average, lower than Nagano's trend would predict. We considered whether measurements at pH 13, as performed by Nagano, would reconcile the observed differenced but, for most part, the fluorescence quantum yields of 1–4 were unchanged at higher pH.
28. Rotman A, Heldman J. Biochemistry. 1981; 20:5995–5999. [PubMed: 7306488]
29. Salic A, Mitchison TJ. Proc Natl Acad Sci. 2008; 105:2415–2420. [PubMed: 18272492]
30. Hong V, Steinmetz NF, Manchester M, Finn MG. Bioconj Chem. 2010; 21:1912–1916.
31. Besanceney-Webler C, Jiang H, Zheng T, Feng L, Soriano del Amo D, Wang W, Klivansky LM, Marlow FL, Liu Y, Wu P. Angew Chem Int Ed. 2011; 50:8051–8056.
32. Hsu TL, Hanson SR, Kishikawa K, Wang SK, Sawa M, Wong CH. Proc Natl Acad Sci. 2007; 104:2614–2619. [PubMed: 17296930] Chang PV, Chen X, Smyrniotis C, Xenakis A, Hu TS, Bertozzi CR, Wu P. Angew Chem Int Ed. 2009; 48:4030–4033.
33. Staros JV, Bayley H, Standring DN, Knowles JR. Biochem Biophys Res Comm. 1978; 80:568–572. [PubMed: 24446]
34. Lippert AR, New EJ, Chang CJ. J Am Chem Soc. 2011; 133:10078–100800. [PubMed: 21671682] Peng H, Chen S, Chen Z, Ren W, Ai H. J Am Chem Soc. 2012; 134:9589–9592. [PubMed: 22642566]

35. Mineno T, Ueno T, Urano Y, Kojima H, Nagano T. Org Lett. 2006; 8:5963–5966. [PubMed: 17165905]

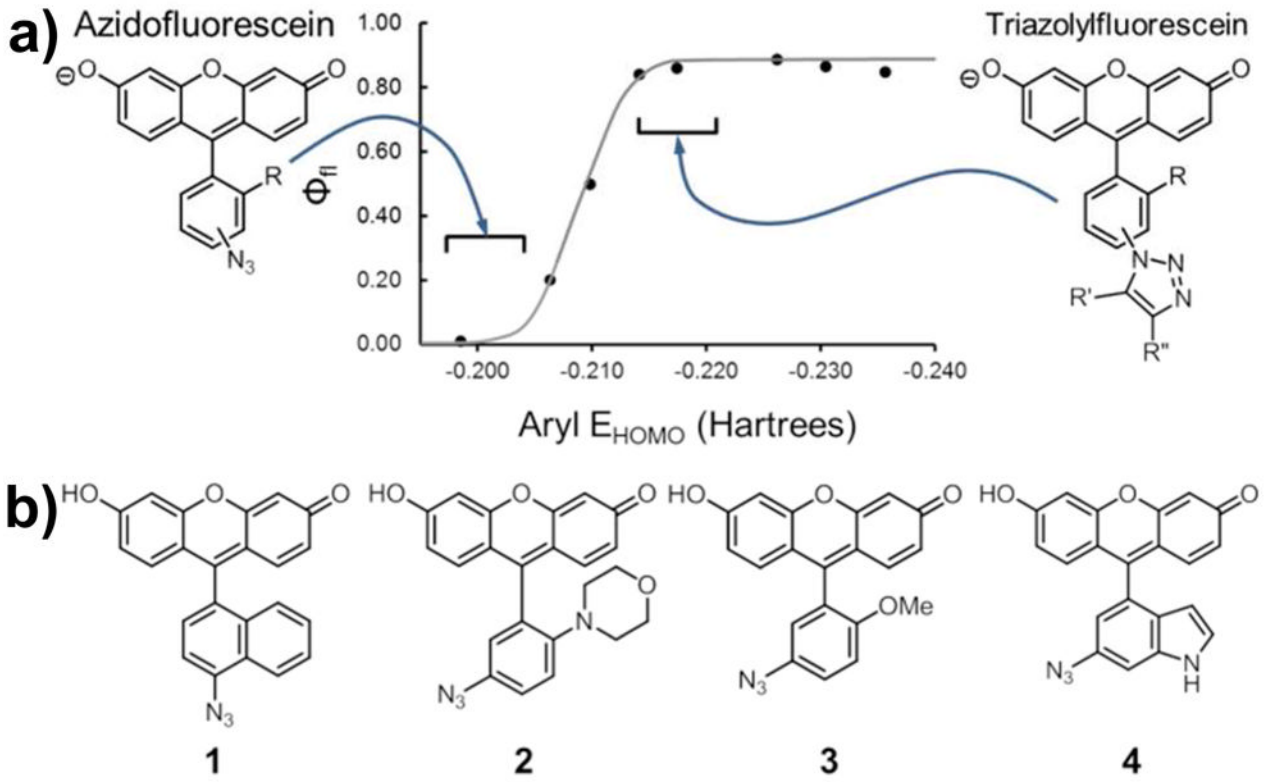

Figure 1.

Computation-aided design of fluorogenic azidofluorescein analogs. **a.** Relationship between pendant aryl E_{HOMO} and fluorescence quantum yield. The ideal E_{HOMO} values of the azido and triazolylfluorescein analogs (left and right, respectively) are indicated with brackets.[14] **b.** Structures of target azidofluoresceins **1–4**.

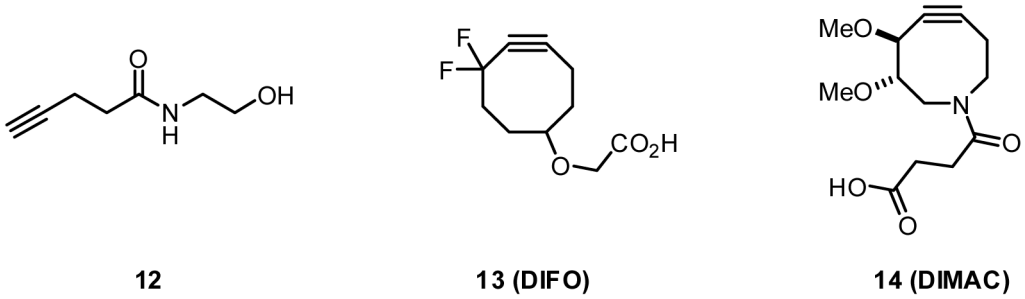

12 **13 (DIFO)** **14 (DIMAC)**

Figure 2.
Alkynes used for triazolylfluorescein synthesis.

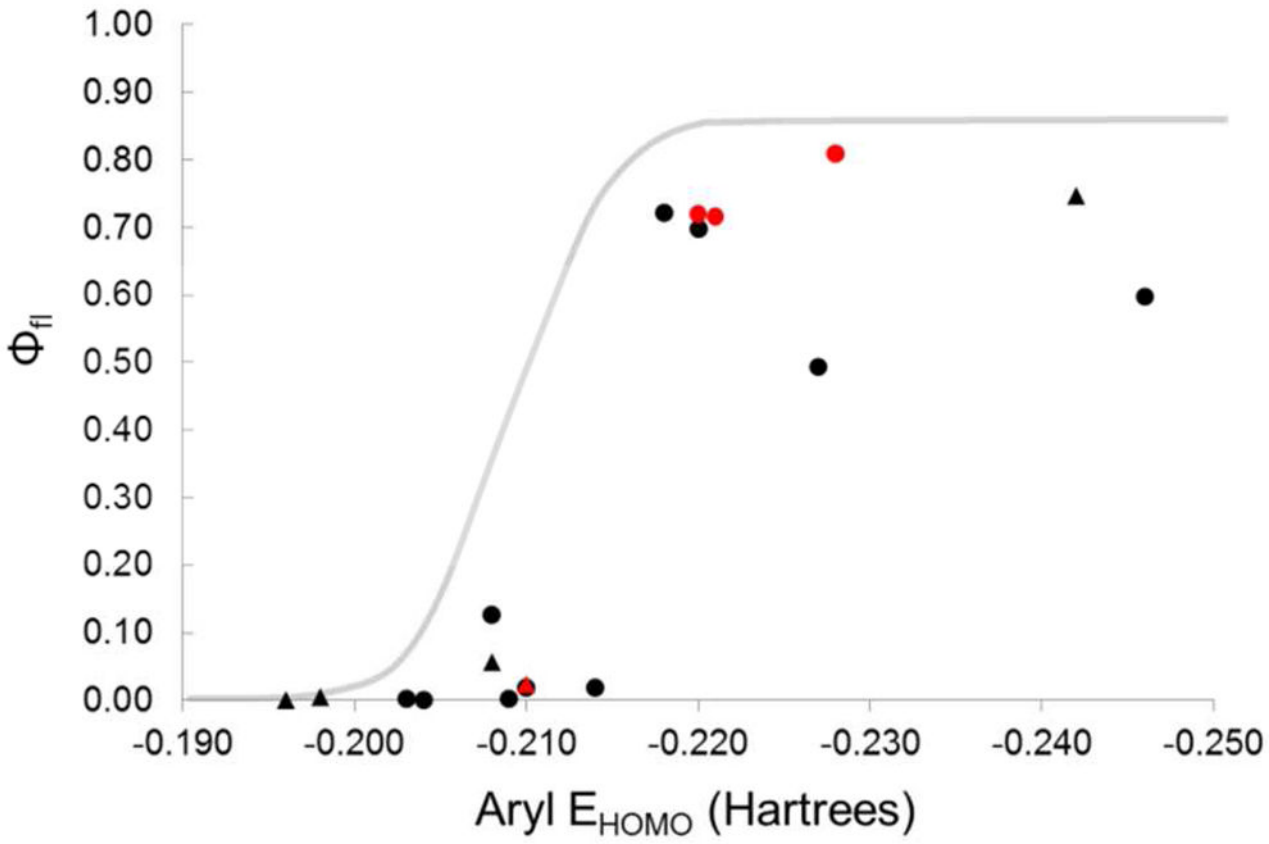

Figure 3.
Relationship between calculated pendant aryl E_{HOMO} and fluorescence quantum yield of azidofluoresceins and triazolylfluoresceins. The grey line denotes the relationship between aryl E_{HOMO} and fluorescence quantum yield determined in Ref. 14. Points represent experimental data from individual azidofluoresceins (triangles) and triazolylfluoresceins (circles). The points corresponding to compound **1** and its triazole products are highlighted in red.

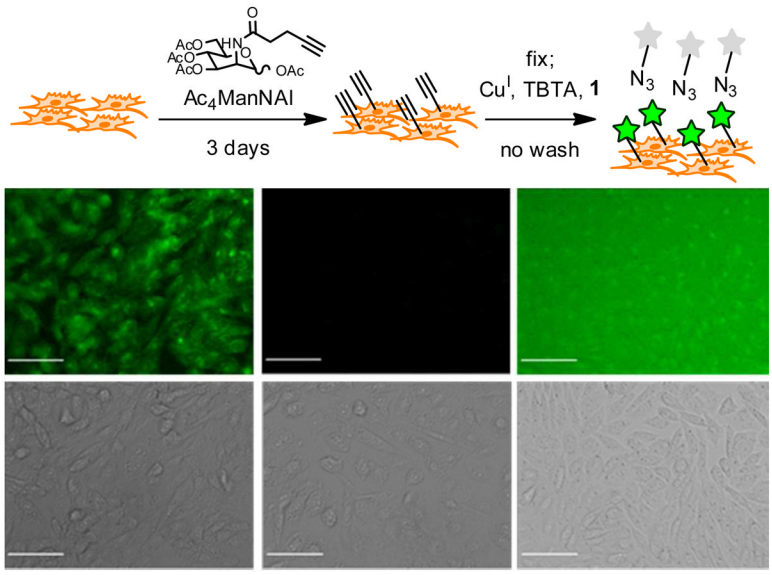

Figure 4. No-wash cell labeling with azidofluorescein probes

a. Outline of the no-wash labeling experiment using Ac_4ManNAl and **1**. CHO cells were metabolically labeled with Ac_4ManNAl or Ac_4ManNAc for 3 d. The cells were then then reacted with 25 μM probe as well as the other reagents for Cu-catalyzed click chemistry for 1 h. **b–g.** Top row: fluorescence images; Bottom row: corresponding DIC images. **b, c.** Ac_4ManNAl-treated cells reacted with **1** (inset shows a 3-fold magnification to highlight cell-surface labeling). **d, e.** Ac_4ManNAc-treated cells reacted with **1. f, g.** Ac_4ManNAl-treated cells reacted with 5-azidofluorescein. Scale bar = 50 μm. Exposure time/ fluorescence cutoffs were 150 ms/150–400 for **b**, **d** and 10 ms/500–900 for **f**.

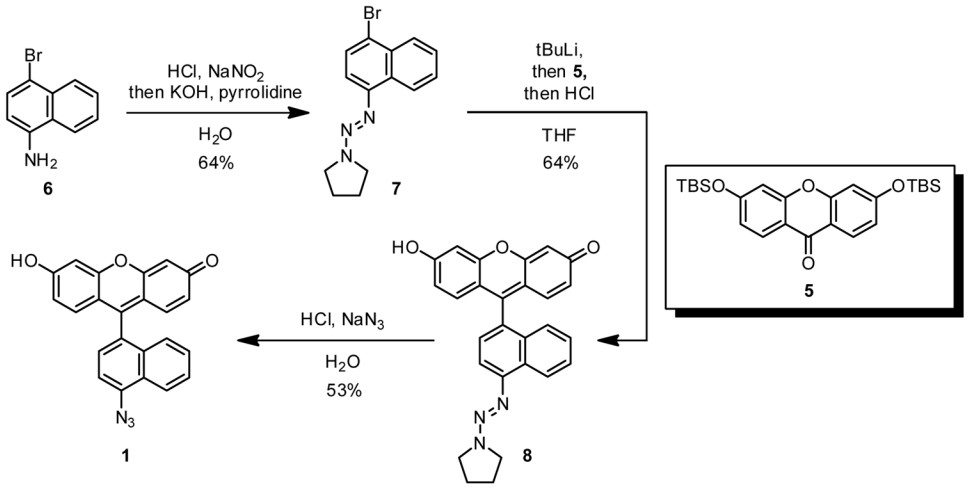

Scheme 1.
Synthesis of azidofluorescein 1.

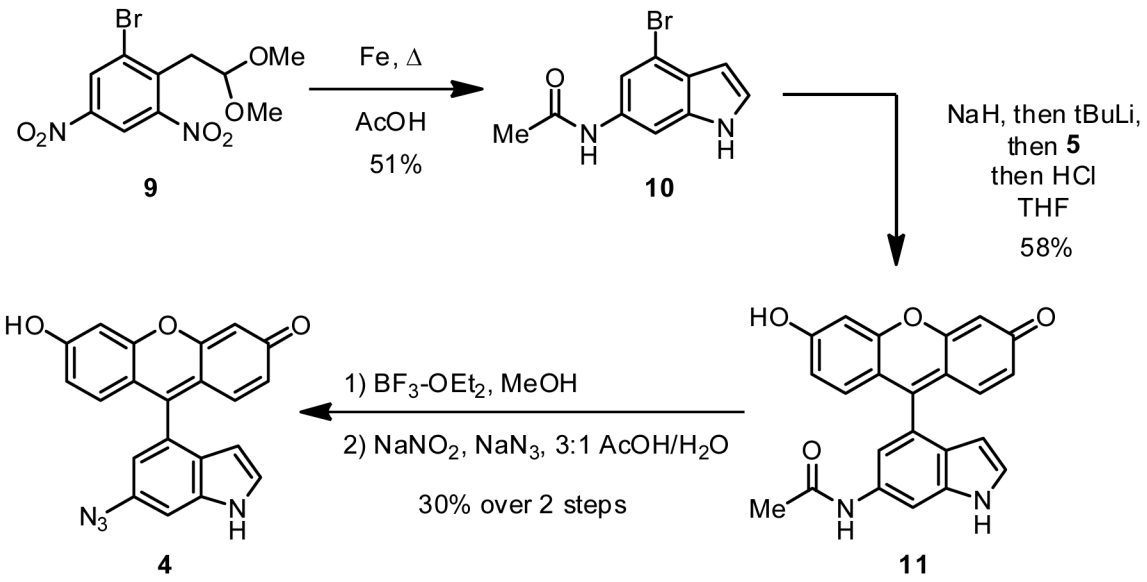

Scheme 2.
Synthesis of azidofluorescein 4.

Table 1

Fluorescence properties of azido- and triazolylfluoresceins in pH 7.4 PBS. "**1–12**" denotes the triazolylfluorescein product from reaction of **1** and **12**. Other triazolylfluoresceins are named analogously

Compound	λ_{ex}	λ_{em}	Φ_{500}	Increase
fluorescein	490	510	--	--
1	497	513	0.024	--
1–12	495	518	0.70	29x
1-DIFO	499	517	0.81	34x
1-DIMAC	499	517	0.72	30x
2	501	521	0.0005 6	--
2–12	506	517	0.0018	3.2x
2-DIFO	507	522	0.0018	3.2x
2-DIMAC	507	521	0.0007 6	1.4x
3	496	516	0.057	--
3–12	499	520	0.72	13x
3-DIFO	499	519	0.49	8.6x
3-DIMAC	499	518	0.72	13x
4	497	518	0.0052	--
4–12	499	519	0.13	25x
4-DIFO	497	520	0.019	3.7x
4-DIMAC	497	516	0.020	3.8x
N_3-fluor	492	511	0.75	--
N_3-fluor-12	494	516	0.59	0.79x